IJE TRANSACTIONS A: Basics Vol. 29, No. 10, (October 2016) 1469-1477

International Journal of Engineering

Journal Homepage: www.ije.ir

RESEARCH NOTE

Two-fluid Electrokinetic Flow in a Circular Microchannel

A. Jabari Moghadam*

Department of Mechanical Engineering, Shahrood University of Technology, Shahrood, Iran

PAPER INFO

Paper history:
Received 29 May 2016
Received in revised form 17 July 2016
Accepted 25 August 2016

Keywords:
Electroosmosis
Pressure-gradient
Two-fluid stratified Flow
Exact Solution

ABSTRACT

The two-fluid flow is produced by the combined effects of electroosmotic force in a conducting liquid and pressure gradient force in a non-conducting liquid. The Poisson-Boltzmann and Navier-Stokes equations are solved analytically; and the effects of governing parameters are examined. Poiseuille number increases with increasing the parameters involved. In the absence of pressure gradient, the two fluids demonstrate plug-like velocity profiles. The results reveal that the two-fluid electroosmotic pumping flow rate is feasible for a relatively small interface zeta potential; or large wall zeta potential and electrokinetic radius. For particular values of the governing parameters, the flow rate approaches a specific value as the electrokinetic radius tends to infinity. A back flow (a negative value of the resultant flow rate) occurs for sufficiently small values of the wall zeta potential or sufficiently large values of the interface zeta potential (even in the case of pressure-assisted flow). Zero-value flow rates may also be attained.

***doi**: 10.5829/idosi.ije.2016.29.10a.18*

NOMENCLATURE

dp/dz	pressure gradient [Pa/m]
e	electron charge [C]
E	axial electrical field strength [V/m]
f	friction factor
$I_\nu(x)$	modified Bessel function of the first kind of order ν
$K_\nu(x)$	modified Bessel function of the second kind of order ν
k_B	Boltzmann constant [J/K]
n_0	bulk ion concentration [m^{-3}]
Po	Poiseuille number
q	liquid-2 flow rate ratio
Q	dimensionless volumetric flow rate
r	radial coordinate [m]
$\Re$	radius of the micro-channel [m]
$\Re_0$	Radius of interface [m]
R	dimensionless radial coordinate
R_0	Dimensionless radius of interface
Re	Reynolds number
T	absolute temperature [K]
U_{Hs}	Helmholtz-Smoluchowski velocity [m/s]
U_{PD}	pressure-driven reference velocity [m/s]
V	dimensionless axial velocity
V_z	axial velocity [m/s]
z	axial coordinate [m]
Z	Dimensionless wall zeta potential
Z_0	dimensionless interface zeta potential
$\aleph$	Valence of ionic species
Greek symbols	
μ	liquid dynamic viscosity [kg/m.s]
τ_{rz}	shear stress [Pa]
τ^*	dimensionless shear stree
χ	the electro-kinetic radius
ε	electric permittivity of solution [F/m]
κ	Debye-Huckel parameter [m^{-1}]
ρ	fluid density [kg/m^3]
ρ_e	net volume charge density [C m^{-3}]
$\bar{\rho}_{ei}^s$	dimensionless interface charge density
ψ	electrical potential [V]
Ψ	dimensionless electrical potential
ζ	zeta potential at the wall [V]
ζ_0	zeta potential at the interface [V]
μ	liquid dynamic viscosity [kg/m.s]
subscripts	
1, 2	conducting , non-conducting liquids

*Corresponding Author's Email: *alijabari@shahroodut.ac.ir* (A. Jabari Moghadam)

Please cite this article as: A. Jabari Moghadam, Two-fluid Electrokinetic Flow in a Circular Microchannel, International Journal of Engineering (IJE), TRANSACTIONS A: Basics Vol. 29, No. 10, (October 2016) 1469-1477

1. INTRODUCTION

Unlike flows in conventional macro-sized channels, the analysis of flow in micro-channels has to take into consideration the presence of the electric double layer (EDL), which is formed as a result of the interaction between the charged wall surface and ionized solution. The fluid is then moved by applying an electric field to the EDL. Since the surface to volume ratio in microscale is large, electroosmotic flow (EOF) would be more efficient than ordinary pressure-driven flows. EOF micropumps contain no moving parts and are relatively easy to integrate in microfluidic circuits during fabrication. Microfluidic devices utilizing EOF have great applications with medical research as well as some other fields such as physics and chemistry (in fuel cells, soil analysis and processing, and chemistry analysis). Understanding the electrokinetic-driven flows in various geometries and the complete control of the flows at micro-scales will allow the construction of highly complex and efficient microsystems, where fluids can circulate in a controlled manner, performing a large number of tasks in a maze of microchannel [1, 2].

Extensive studies have been conducted to explore the behavior of electro-osmotic flow in micro-scale devices. Squires and Bazant [3] described the general phenomenon of induced-charge electro-osmosis (ICEO) which includes a wide variety of techniques for driving micro-flows around conducting or dielectric surfaces using AC or DC electric fields. Arulanandam and Li [4] studied the liquid movement in a rectangular micro-channel by electro-osmotic pumping. They used a 2D Poisson-Boltzmann equation and the 2D momentum equation to model the problem. The flow field and volumetric flow rate were presented as functions of the zeta potential, the ionic concentration, the aspect ratio, and the applied electrical field. Dutta and Beskok [5] presented analytical results for velocity distribution, mass flow rate, pressure gradient, wall shear stress, and vorticity in mixed electro-osmotic/pressure driven flows for two-dimensional straight channel geometry. Tang et al. [6] investigated the electro-osmotic flow in axisymmetric micro-ducts. They presented axisymmetric lattice Boltzmann models to solve the electric potential distribution and the velocity field. Wang and Kang [7] presented a numerical solution based on coupled lattice Boltzmann methods for electro-kinetic flows in micro-channels. Xuan and Li [8] used a semi-analytical approach to investigate electro-osmotic flows in micro-channels with arbitrary cross-sectional geometry and distribution of wall charge. Kang et al. [9] solved the electro-osmotic flow problem in a cylindrical channel for only sinusoidal waveform by the Green's function method. Tsao [10] studied the electroosmotic flow through an annulus under the constant electric field condition. Kang et al. [11] investigated the steady-state electroosmotic flow in a capillary annulus under the situation when the two cylindrical walls carry high zeta potentials. In their study, the non-linear term of the Poisson-Boltzmann equation (i.e. hyperbolic sine) has been approximated by some proposed relations.

Erickson and Li [12] presented a combined theoretical and numerical approach to investigate the time periodic electro-osmotic flow in a rectangular micro-channel. Comprehensive models for a slit channel have also been presented by Dutta and Beskok [13] who developed an analytical model for an applied sinusoidal electric field. Green et al. [14] experimentally observed peak flow velocities on the order of hundreds of micrometers per second near a set of parallel electrodes subject to two AC fields, 180 degrees out-of-phase with each other. The effect was subsequently modeled using a linear double layer analysis by Gonzalez et al. [15]. Using a similar principal, both Brown et al. [16] and Studer et al. [17] presented microfluidic devices that incorporated arrays of non-uniformly sized embedded electrodes which, when subject to an AC field, were able to generate a bulk fluid motion. Moghadam [18-20] obtained exact solutions of AC electroosmotic flows in circular and annular microchannels by using the Green's function method. The flow fields excited by various time-periodic electric currents were also examined. Moghadam and Akbarzadeh [21] examined time-periodic EOF of a non-Newtonian fluid in microchannels using a numerical scheme. Also, the problem of thermally-developing electroosmotic flow in a circular microchannel [22] was studied under DC electric field; and some analytic solutions were obtained. Wang et al. [23] studied the mixing enhancement by the electroosmotic flow in microchannels using the Lattice-Boltzmann methods. Also, the numerical results of electroosmotic flows in micro- and nanofluidics using a Lattice Poisson-Boltzmann method were presented [24] to solve the non-linear governing equations.

Some liquids, such as non-polar fluids with very low electrical conductivity, cannot form EDLs; hence, they cannot be directly pumped using electroosmosis. A conducting pumping liquid driven by EOF can pull a non-conducting working fluid by viscous forces. In some biochemical analysis, on the other hand, EOF pumps may not be suitable to be used directly with the water solutions, because the voltage applied can lead to electrochemical decomposition of the solute, fluctuation of the buffer solution pH and generation of gases [25]. In these cases, an EOF, which is driven thru layers of the conducting liquid, is utilized to pump a non-conducting liquid. This allows for new types of analysis in the field of micro Total Analysis Systems (μTAS) which may prove important in the drug industry and for environmental monitoring. The characteristics flow rate and pressure of the pump are in the range of nL/s and kPa, respectively; but depends largely on geometrical as well as electrical properties. In order to drive low EO mobility liquids and also avoid the aforementioned problems, Brask et al. [26] and Watanabe et al. [25], independently, proposed the idea of using high EO mobility liquids as driving mechanism to drag another fluid. The flow of two immiscible fluids was modeled by Ngoma and Erchiqui [27] in a parallel-plate microchannel; and the effects of pressure gradient and electroosmosis were studied. Gao et al. [28] studied two-fluid EOF in a rectangular microchannel, and examine the effects of various variables on the flow field. Analytic solutions of transient electroosmotic and pressure-driven flow of two-layer fluids was obtained by Su et al. [29] and Gao et al. [30] in slit and rectangular microchannels, respectively. Stiles et al. [31] proposed a simple method to focus the sample stream by using either a single suction pump or capillary pumping effect. The focused stream width was controlled by varying the relative resistances of the side and inlet channel flows. Fu at al. [32] presented experimental and numerical results electrokinetic flow injection. By applying different voltages at different parts of the channel, the sample fluid can be directed into a specific outlet channel. An analytical model was presented by Afonso at al. [33] to describe a two-fluid electroosmotic flow of Newtonian and viscoelastic fluids in a planar microchannel.

While the previous studies consider the flow in microtubes under various conditions, there is a distinct lack of discussion on the hydrodynamic behavior of the combined electroosmotic and pressure-driven flow in circular microchannels. This paper presents an analytic solution of two-fluid EOF in a circular microchannel which is driven by electroosmosis and pressure gradient effects; the surface charge at the liquid-liquid interface is also taken into account. This EOF pump consists of two immiscible liquids: a high EO mobility or conducting liquid near the channel wall and a low EO mobility or non-conducting liquid around the channel centerline. The liquid-liquid interface has excess surface charge density. The applied external electric field interacts with net charges within the double layers (at the wall and at the interface) and creates an electroosmotic body force on the bulk conducting liquid; a pressure gradient may also be applied across the non-conducting liquid. The non-conducting liquid is delivered by the applied pressure gradient force as well as the interfacial viscous force of the conducting liquid driven by electroosmosis. The resultant body force drives the two-liquid field whose characteristics depend on the relative intensity of each body force.

2. GOVERNING EQUATIONS AND SOLUTIONS

A circular microchannel is filled with two immiscible fluids (illustrated in Figure 1), in which, the inner fluid is a non-conducting liquid and the outer fluid is a conducting liquid. Electric double layers form at the wall as well as at the liquid-liquid interface, which are in contact with the high EO mobility liquid. The zeta potential at the wall and at the interface are ζ and ζ_0, respectively. The electroosmosis body force (applied on the liquid 1) and the pressure-gradient body force (applied on the liquid 2) are along the z-direction.

2. 1. Potential Field The electric potential distribution for a symmetric electrolyte due to the presence of EDL is determined by the Poisson-Boltzmann equation [34, 35]:

$$\frac{d^2\psi}{dr^2}+\frac{1}{r}\frac{d\psi}{dr}=\frac{2\aleph e n_0}{\varepsilon}\sinh\left(\frac{\aleph e\psi}{k_B T}\right) \tag{1}$$

where, ψ, $\aleph$, e, n_0, ε, k_B, and T are the electrical potential, the valence, the electron charge, the bulk ion concentration, the electric permittivity of the electrolyte, the Boltzmann constant, and the absolute temperature, respectively. The boundary conditions are:

$$\psi(r=\Re)=\zeta \tag{2a}$$

$$\psi(r=\Re_0)=\zeta_0 \tag{2b}$$

Introducing the following dimensionless variables:

$$R=\frac{r}{\Re} \quad , \quad \Psi=\frac{\aleph e}{k_B T}\psi \tag{3}$$

and under the Debye-Huckel approximation $\left(|\aleph e\zeta|<k_B T\right)$, we write Equation (1) in dimensionless form as follows:

$$\frac{d^2\Psi}{dR^2}+\frac{1}{R}\frac{d\Psi}{dR}=\chi^2\Psi \tag{4}$$

in which, $\chi=\kappa\Re$ is the electrokinetic radius (the length scale ratio); κ is the Debye-Huckel parameter defined as:

$$\kappa=\left(\frac{2\aleph^2 e^2 n_0}{\varepsilon k_B T}\right)^{1/2} \tag{5}$$

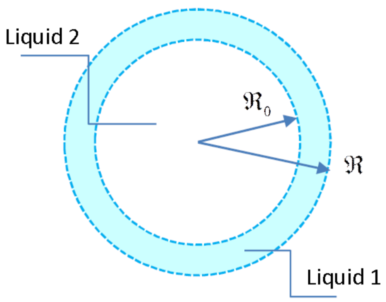

Figure 1. cross-section of the two-fluid microchannel

The boundary conditions (2) in dimensionless form are:

$$\Psi(R=1)=Z \tag{6a}$$

$$\Psi(R=R_0)=Z_0 \tag{6b}$$

It is noted that $0<R_0<1$. Solution of (4) subjected to (6) is:

$$\Psi(R)=\frac{K_0(\chi R)\left[Z_0 I_0(x)-Z I_0(\chi R_0)\right]-I_0(\chi R)\left[Z_0 K_0(\chi)-Z K_0(\chi R_0)\right]}{K_0(\chi R_0)I_0(\chi)-K_0(\chi)I_0(\chi R_0)} \tag{7}$$

It should be noted that the electric potential for $0\le R<R_0$ is zero; while it is specified by Equation (7) for $R_0\le R\le 1$.

2. 2. Velocity Field It is assumed that the two immiscible liquids are Newtonian; so the fully-developed EOF for the conducting liquid is described by the following simplified momentum equation [34, 35]:

$$\mu_1\left(\frac{\partial^2 V_{z1}}{\partial r^2}+\frac{1}{r}\frac{\partial V_{z1}}{\partial r}\right)=-2\aleph e n_0\sinh\left(\frac{\aleph e\psi}{k_B T}\right)E_z \tag{8}$$

where, V_{z1} is the only non-zero velocity component of liquid 1 along the microchannel, μ_1 is the viscosity of liquid 1, and E_z is the electric field strength. For the non-conducting liquid, the momentum equation gives:

$$\mu_2\left(\frac{\partial^2 V_{z2}}{\partial r^2}+\frac{1}{r}\frac{\partial V_{z2}}{\partial r}\right)=\frac{dp}{dz} \tag{9}$$

At the interface $(r=\Re_0)$, matching conditions must be satisfied. They are the continuities of velocity and shear stress which are represented as:

$$\left\{\begin{aligned} &V_{z1}=V_{z2}\\ &\mu_1\frac{\partial V_{z1}}{\partial r}=\mu_2\frac{\partial V_{z2}}{\partial r}+E_z\rho_{ei}^s\end{aligned}\right\}_{\text{at } r=\Re_0} \tag{10}$$

in which, the interface charge density, ρ_{ei}^s, is calculated from:

$$\rho_{ei}^s=-\varepsilon\frac{\partial\psi}{\partial r}(r=\Re_0)\quad \underline{\text{in dimensionless form}}\quad \bar{\rho}_{ei}^s=-\frac{\partial\Psi}{\partial R}(R=R_0) \tag{11}$$

The latter can be determined by differentiating Equation (7) evaluated at $R=R_0$:

$$\bar{\rho}_{ei}^s=\frac{\chi\left\{I_1(\chi R_0)\left[Z_0K_0(\chi)-ZK_0(\chi R_0)\right]+K_1(\chi R_0)\left[Z_0I_0(\chi)-ZI_0(\chi R_0)\right]\right\}}{K_0(\chi R_0)I_0(\chi)-K_0(\chi)I_0(\chi R_0)} \tag{12}$$

To non-dimensionalize Equations (8)-(10), we would introduce Equation (3) together with the following reference quantities:

$$V_1=\frac{V_{z1}}{U_{HS}},\qquad V_2=\frac{V_{z2}}{U_{HS}}$$
$$E=\frac{E_zL}{\zeta},\qquad \Gamma=\frac{U_{PD}}{U_{HS}} \tag{13}$$

where, L is the distance between the two electrodes, Γ is the body force ratio, U_{PD} and U_{HS} are the pressure-driven and Helmholtz-Smoluchowski reference velocities, respectively, expressed by:

$$U_{PD}=\frac{\Re^2}{4\mu_2}\left(-\frac{dp}{dz}\right)\quad;\quad U_{HS}=\frac{\varepsilon k_BTE_z}{\aleph e\mu_1} \tag{14}$$

Then, Equations (8)-(10) become:

$$\frac{d^2V_1}{dR^2}+\frac{1}{R}\frac{dV_1}{dR}+\chi^2\Psi=0 \tag{15}$$

$$\frac{d^2V_2}{dR^2}+\frac{1}{R}\frac{dV_2}{dR}+4\Gamma=0 \tag{16}$$

$$\left\{\begin{aligned} &V_1=V_2\\ &\frac{dV_1}{\partial R}=\mu_{21}\frac{dV_2}{\partial R}+\bar{\rho}_{ei}^s\end{aligned}\right\}_{R=R_0} \tag{17}$$

in which, μ_{21} is called the viscosity ratio. There are, in addition, two further boundary conditions:

$$V_1(R=1)=0\quad,\quad \frac{dV_2}{dR}(R=0)=0 \tag{18}$$

Equations (15) and (16) are now solved with respect to boundary conditions (17) and (18).

$$\begin{aligned}V_1(R)=&Z-2\Gamma\mu_{21}R_0^2\ln(R)\\&+\frac{I_0(\chi R)\left[Z_0K_0(\chi)-ZK_0(\chi R_0)\right]+K_0(\chi R)\left[ZI_0(\chi R_0)-Z_0I_0(\chi)\right]}{K_0(\chi R_0)I_0(\chi)-K_0(\chi)I_0(\chi R_0)}\end{aligned} \tag{19}$$

$$V_2(R)=\Gamma\left[R_0^2\left(1-2\mu_{21}\ln(R_0)\right)-R^2\right]+Z-Z_0 \tag{20}$$

One the flow field is determined, the Poiseuille number (Po), the non-dimensional volumetric flow rate (Q), and the liquid-2 flow rate ratio (q) can be obtained by the following formula:

$$Po=f\,.\mathrm{Re}=2\tau_W^*\big|_{R=1} \tag{21}$$

$$Q=Q_1+Q_2=\int_{R_0}^{1}RV_1dR+\int_0^{R_0}RV_2dR \tag{22}$$

$$q=Q_2/Q \tag{23}$$

in which, $f=2\tau_w/\left(\rho_1U_{HS}^2\right)$, $\mathrm{Re}=\rho_1U_{HS}\Re/\mu_1$ and $\tau^*=\tau_{rz}/\left(\mu_1U_{HS}/\Re\right)=-\partial V_1/\partial R$. The above quantities are presented below:

$$\begin{aligned}Po=&2\Gamma\mu_{21}R_0^2\\&+\frac{\chi\left\{I_1(\chi)\left[Z_0K_0(\chi)-ZK_0(\chi R_0)\right]+K_1(\chi)\left[Z_0I_0(\chi)-ZI_0(\chi R_0)\right]\right\}}{K_0(\chi)I_0(\chi R_0)-K_0(\chi R_0)I_0(\chi)}\end{aligned} \tag{24}$$

$$\begin{aligned}Q=&\frac{Z}{2}+\frac{R_0^2}{2}\left(\Gamma\mu_{21}-Z_0\right)+\frac{R_0^4}{4}\Gamma\left(1-2\mu_{21}\right)\\&+\frac{Nume.}{K_0(\chi R_0)I_0(\chi)-K_0(\chi)I_0(\chi R_0)}\end{aligned} \tag{25}$$

$$
\begin{aligned}
Nume. = {} & R_0 K_1(\chi R_0)\left[Z I_0(\chi R_0) - Z_0 I_0(\chi)\right] \\
& + R_0 I_1(\chi R_0)\left[Z K_0(\chi R_0) - Z_0 K_0(\delta)\right] \\
& + I_1(\chi)\left[Z_0 K_0(\chi) - Z K_0(\chi R_0)\right] \\
& + K_1(\chi)\left[Z_0 I_0(\chi) - Z I_0(\chi R_0)\right]
\end{aligned} \tag{26}
$$

$$
q = \frac{R_0^2}{4Q}\left\{2(Z - Z_0) + \Gamma R_0^2\left[1 - 4\mu_{21}\ln(R_0)\right]\right\} \tag{27}
$$

3. Results and Discussion

The effects of non-dimensional governing parameters on the hydrodynamic features of two-fluid electroosmotically and pressure-driven flow are examined in a circular micrichannel. A non-conducting liquid (low EO fluid) holds the central portion of the channel, and a conducting liquid (high EO fluid) holds the area close to the wall. The normalized zeta potentials (at the wall and at the interface) are selected within the bounds imposed by the Debye-Hückel linearization. The characteristic scale of the microchannel to Debye length (the electrokinetic radius) is considered in the range of $\chi = 100 - 1000$ to investigate the essential features of EOF in a $100\mu m$ microchannel.

Figure 2a shows the non-dimensional potential distribution in the microchannel cross-sectional area for two different values of χ. Two electric double layers, close to the wall and near the liquid-liquid interface, are formed in the high EO mobility liquid due to the existence of wall and interfacial zeta potentials, respectively. The value of χ determines the EDL thickness; a larger value of χ (a larger bulk-ionic concentration and/or a larger channel size) corresponds to a thinner EDL. Figures 2a and 2b may be comparable with Figures 3b and 5a, respectively, in [28]; and show similar trends. The flow velocity of the conducting fluid (Figure 2c) was favorably compared with Figure 1b in [25] achieved using the analytic approach employed for a single conducting fluid flow thru a circular microchannel.

The two-liquid flow is driven by the pressure-gradient body force of the non-conducting liquid as well as the electric body/surface force of conducting liquid. It is noted that the electric body force results from the interaction of the external electric field with the volumetric local net charges in the high EO mobility liquid, while, the electric surface force is due to the effect of the external electric field on the interface free charges.

The combined effects of driving forces on dimensionless velocity profiles of the two liquids are illustrated in Figure 3.

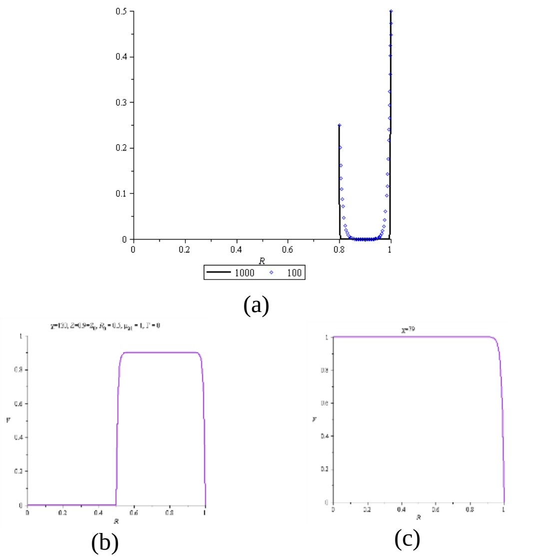

Figure 2. (a) Dimensionless potential distributions for $R_0 = 0.8$, $Z = 0.5$, $Z_0 = 0.25$ and two values of χ, (b) and (c) Dimensionless velocity profiles for comparison

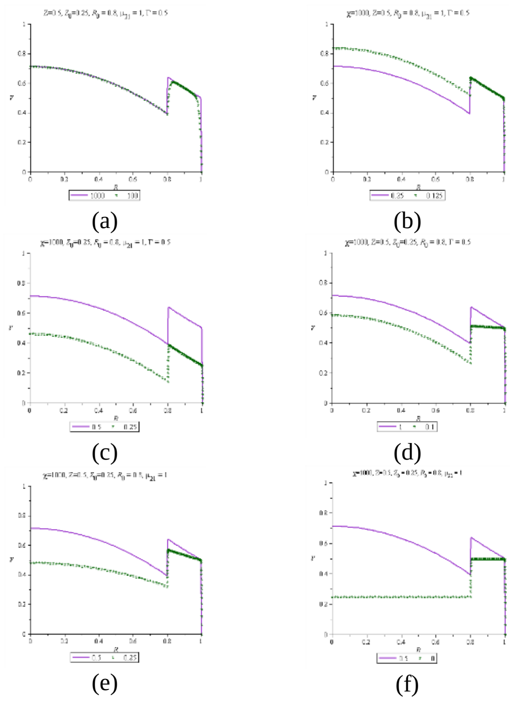

Figure 3. Variations of non-dimensional velocity profiles with (a) χ (b) Z_0 (c) Z (d) μ_{21} (e) Γ (f) Γ

As shown in Figure 3a, higher electrokinetic radius corresponds to higher velocity gradients at the wall and at the interface; also, maximum velocity within the EDL increases. Figure 3b shows that a decrease in Z_0 causes the velocity of liquid 2 to increase, since the surface charges at the interface generate a force acting in the opposite direction to the EOF body force in the EDL region at the vicinity of the interface. When zeta potential at the wall is decreased (Figure 3c), the flow velocity is obviously decreases. When μ_{21} is high, the flow resistance of the non-conducting liquid is higher than that of the conducting liquid, hence maximum velocity of liquid 1 is enhanced and so its velocity gradient (Figure 3d). In the case of small viscosity ratio, the non-conducting liquid is relatively easy to be dragged by the conducting liquid, and therefore the velocity gradient of liquid 1 reduces. Figure 3e demonstrates that larger Γ results in higher values of velocity, as well as a larger curvature of liquid-2 profile and a steeper incline of liquid-1 profile. Effect of $\Gamma = 0$, as illustrated in Figure 3f, is to produce plug-like velocity profiles for both liquids (independent of μ_{21} selection).

Variations of the Poiseuille number versus χ and Z are illustrated in Figure 4. It can be seen that increasing χ has the same effect as Z which is increasing the Poiseuille number. By increasing χ, the Debye length is reduced, resulting in a higher velocity gradient inside the EDL and consequently a more Poiseuille number. The Poiseuille number value grows by increasing Z too, since higher electroosmotic force and therefore larger velocity gradient within the EDL will be produced.

Variables R_0, μ_{21} and Γ have also increasing effects on the Poiseuille number (Figure 5). According to Equation (24), Po has a linear relationship with μ_{21} and Γ and almost a quadratic relationship with R_0. All these variables cause the velocity gradient inside the Debye length to increase, hence Po increases.

Figure 6 depicts dimensionless volumetric flow rate as a function of χ, Z, Z_0, R_0, μ_{21} and Γ. As can be seen in Figure 6a, for each individual set of data, the two-fluid flow rate approaches a specific value as $\chi \to \infty$; for instance, $Q \cong 0.2788$ for set of given parameters $Z = 0.5$, $Z_0 = 0.25$, $R_0 = 0.8$, $\mu_{21} = 1$, and $\Gamma = 0.5$.

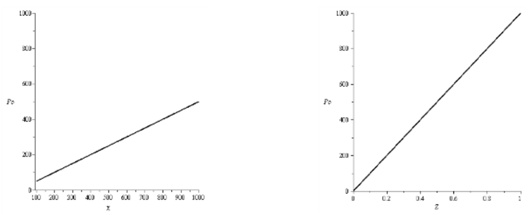

(a) (b)

Figure 4. Poiseuille number against (a) χ with $Z = 0.5$, and (b) Z with $\chi = 1000$ for $Z_0 = 0.25$, $R_0 = 0.8$, $\mu_{21} = 1$ and $\Gamma = 0.5$

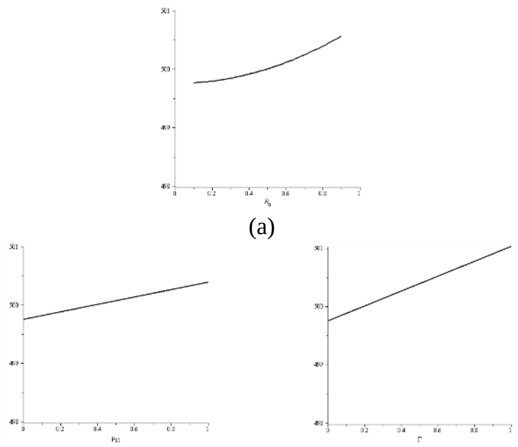

(a) (b) (c)

Figure 5. Poiseuille number against (a) R_0 with $\mu_{21} = 1$ and $\Gamma = 0.5$, (b) μ_{21} with $R_0 = 0.8$ and $\Gamma = 0.5$ and (c) Γ with $R_0 = 0.8$ and $\mu_{21} = 1$ for $\chi = 1000$, $Z_0 = 0.25$

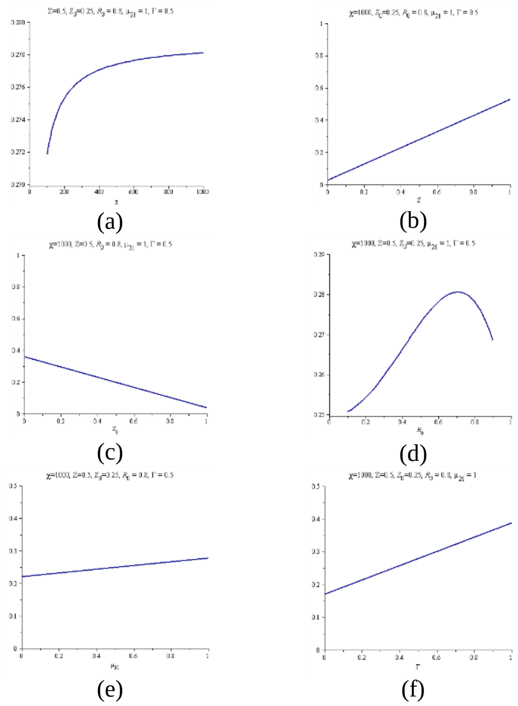

(a) (b) (c) (d) (e) (f)

Figure 6. Variations of volumetric flow rate with (a) χ (b) Z (c) Z_0 (d) R_0 (e) μ_{21} and (f) Γ

The flow rate has an ascending behavior with the wall zeta potential (Figure 6b), since higher electroosmotic force is produced by increasing Z; on the contrary, an increase of Z_0 causes a decrease in Q due to generating an opposite force (Figure 6c). An increase of R_0 may increase or decrease the flow rate, depending on Γ.

Interestingly, in this case, there are two values of R_0 which produce the same flow rate (Figure 6d). Figures 6e and 6f show that increasing μ_{21} and Γ cause the flow rate to increase. Higher μ_{21} means relatively lower viscosity and so higher velocity of liquid 1; higher Γ means relatively higher velocity of liquid 2.

Effects of parameters involved in liquid-2 flow rate ratio are illustrated in Figure 7. The non-conducting liquid is slightly affected by χ and Z. Figure 7c shows that Z_0 has descending influence on q, because the interface free charges induce a resistance to the flow and cause a smaller flow rate of the non-conducting liquid. For some special value of Z_0, q will be zero; and beyond that particular Z_0, a reversing flow will be observed. As shown in Figure 7d, the proportion of non-conducting liquid is obviously increased with increasing R_0. When μ_{21} increases, the relative importance of non-conducting liquid viscosity increases (or conducting liquid viscosity decreases); as liquids 1 and 2 are driven by electroosmosis and pressure-gradient, respectively, the combined effect is to enhance the liquid-2 flow rate slightly (Figure 7e). Liquid 2 is directly influenced by Γ, and its flow rate increases with increasing the body force ratio.

The volumetric flow rate may be negative for sufficiently small values of Z or sufficiently large values of Z_0 (Figure 8).

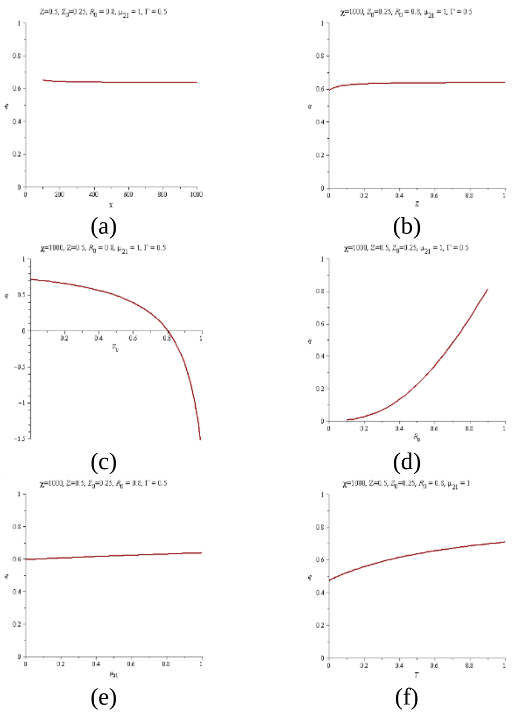

Figure 7. Variations of the liquid-2 flow rate ratio with (a) χ (b) Z (c) Z_0 (d) R_0 (e) μ_{21} and (f) Γ

At some special values of Z and Z_0 where $Q=0$, the q curves demonstrate singularities due to diminishing the denominator of Equation (23).

4. CONCLUSIONS

Analytic solutions of linear Poisson-Boltzmann and Navier-Stokes equations are obtained in a circular microchannel, considering the electroosmosis-driven force and the pressure-driven force as body forces in a conducting and non-conducting incompressible fluids, respectively. The flow behavior depends on the coupling effect between the two liquids. The external electric intensity interacts with the free charges at the liquid-liquid interface to generate a surface force. Upon the application of the electric field, the flow is activated in regions close to the channel wall and the interface. The results of the current research are summarized below:

I. Larger values of electrokinetic radius correspond to smaller values of Debye length and higher velocity gradients near the wall; this leads to larger electroosmotic forces.

II. The interaction between the interface free charges and the external electric field produces a force acting in the opposite direction to the electroosmotic body force in the EDL.

III. A steeper velocity gradient is observed in the conducting liquid for higher viscosity ratio.

IV. An increase in the body force ratio results in increasing the flow velocity, and also curving the non-conducting fluid velocity profile and inclining the conducting fluid velocity profile.

V. When body force ratio is zero, both liquids attain plug-like velocity profiles.

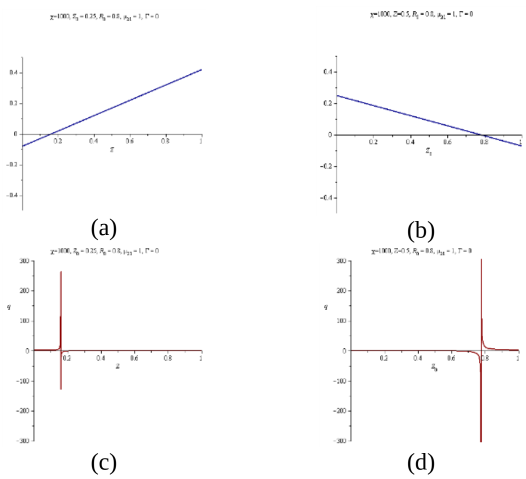

Figure 8. Variations of volumetric flow rate with (a) Z and (b) Z_0, and variations of the liquid-2 flow rate ratio with (c) Z and (d) Z_0

VI. Poiseuille number is an increasing function of electrokinetic radius, wall zeta potential, interface radius, viscosity ratio, and body force ratio.

VII. Dimensionless volumetric flow rate approaches a specific value as $\chi \to \infty$ (for the parameters involved). It is enhanced with increasing the wall zeta potential, while an opposite trend is observed with increasing the interface zeta potential. The flow rate may have ascending or descending trend with the interface radius, depending on the body force ratio. Viscosity ratio and body force ratio both are means of flow rate enhancement. For sufficiently small values of the wall zeta potential or sufficiently large values of the interface zeta potential, the volumetric flow rate may become negative (an entirely back flow). A zero flow rate is clearly attainable.

VIII. Beyond some particular value of the interface zeta potential, a back flow may be observed.

IX. The proportion of non-conducting liquid flow rate is enhanced by increasing the viscosity ratio as well as the body force ratio.

5. REFERENCES

1. Nguyen, N.-T. and Wereley, S.T., "Fundamentals and applications of microfluidics, Artech House, (2002).
2. Tabeling, P., "Introduction to microfluidics, Oxford University Press on Demand, (2005).
3. Squires, T.M. and Bazant, M.Z., "Induced-charge electro-osmosis", ***Journal of Fluid Mechanics***, Vol. 509, (2004), 217-252.
4. Arulanandam, S. and Li, D., "Liquid transport in rectangular microchannels by electroosmotic pumping", ***Colloids and Surfaces A: Physicochemical and Engineering Aspects***, Vol. 161, No. 1, (2000), 89-102.
5. Dutta, P. and Beskok, A., "Analytical solution of combined electroosmotic/pressure driven flows in two-dimensional straight channels: Finite debye layer effects", ***Analytical chemistry***, Vol. 73, No. 9, (2001), 1979-1986.
6. Tang, G., Li, X. and Tao, W., "Microannular electro-osmotic flow with the axisymmetric lattice boltzmann method", ***Journal of Applied Physics***, Vol. 108, No. 11, (2010), 114903.
7. Wang, M. and Kang, Q., "Modeling electrokinetic flows in microchannels using coupled lattice boltzmann methods", ***Journal of Computational Physics***, Vol. 229, No. 3, (2010), 728-744.
8. Xuan, X. and Li, D., "Electroosmotic flow in microchannels with arbitrary geometry and arbitrary distribution of wall charge", ***Journal of colloid and interface science***, Vol. 289, No. 1, (2005), 291-303.
9. Kang, Y., Yang, C. and Huang, X., "Dynamic aspects of electroosmotic flow in a cylindrical microcapillary", ***International Journal of Engineering Science***, Vol. 40, No. 20, (2002), 2203-2221.
10. Tsao, H.-K., "Electroosmotic flow through an annulus", ***Journal of Colloid and Interface Science***, Vol. 225, No. 1, (2000), 247-250.
11. Kang, Y., Yang, C. and Huang, X., "Electroosmotic flow in a capillary annulus with high zeta potentials", ***Journal of Colloid and Interface Science***, Vol. 253, No. 2, (2002), 285-294.
12. Erickson, D. and Li, D., "Analysis of alternating current electroosmotic flows in a rectangular microchannel", ***Langmuir***, Vol. 19, No. 13, (2003), 5421-5430.
13. Dutta, P. and Beskok, A., "Analytical solution of time periodic electroosmotic flows: Analogies to stokes' second problem", ***Analytical Chemistry***, Vol. 73, No. 21, (2001), 5097-5102.
14. Green, N.G., Ramos, A., Gonzalez, A., Castellanos, A. and Morgan, H., "Electric field induced fluid flow on microelectrodes: The effect of illumination", ***Journal of Physics D: Applied Physics***, Vol. 33, No. 2, (2000), 4011-4018.
15. Gonzalez, A., Ramos, A., Green, N.G., Castellanos, A. and Morgan, H., "Fluid flow induced by non-uniform ac electric fields in electrolytes on microelectrodes ii: A linear double layer analysis", ***Physical Review E***, (2000), 4019-4028.
16. Brown, A., Smith, C. and Rennie, A., "Pumping of water with ac electric fields applied to asymmetric pairs of microelectrodes", ***Physical Review E***, Vol. 63, No. 1, (2000), 1-8.
17. Studer, V., Pepin, A., Chen, Y. and Ajdari, A., "Fabrication of microfluidic devices for ac electrokinetic fluid pumping", ***Microelectronic Engineering***, Vol. 61, (2002), 915-920.
18. Moghadam, A.J., "An exact solution of ac electro-kinetic-driven flow in a circular micro-channel", ***European Journal of Mechanics-B/Fluids***, Vol. 34, (2012), 91-96.
19. Moghadam, A.J., "Exact solution of ac electro-osmotic flow in a microannulus", ***Journal of Fluids Engineering***, Vol. 135, No. 9, (2013), 091201.
20. Moghadam, A.J., "Effect of periodic excitation on alternating current electroosmotic flow in a microannular channel", ***European Journal of Mechanics-B/Fluids***, Vol. 48, (2014), 1-12.
21. Moghadam, A.J. and Akbarzadeh, P., "Time-periodic electroosmotic flow of non-newtonian fluids in microchannels", ***International Journal of Engineering-Transactions B: Applications***, Vol. 29, No. 5, (2016), 736-744.
22. Moghadam, A.J., "Thermally developing flow induced by electro-osmosis in a circular micro-channel", ***Arabian Journal for Science and Engineering***, Vol. 39, No. 2, (2014), 1261-1270.
23. Wang, J., Wang, M. and Li, Z., "Lattice boltzmann simulations of mixing enhancement by the electro-osmotic flow in microchannels", ***Modern Physics Letters B***, Vol. 19, No. 28n29, (2005), 1515-1518.
24. Wang, J., Wang, M. and Li, Z., "Lattice poisson–boltzmann simulations of electro-osmotic flows in microchannels", ***Journal of Colloid and Interface Science***, Vol. 296, No. 2, (2006), 729-736.
25. Watanabe, M., Shirai, H. and Hirai, T., "Liquid–liquid two-layer electrohydrodynamic flow system", ***Sensors and Actuators B: Chemical***, Vol. 94, No. 3, (2003), 267-270.
26. Brask, A., Goranovic, G. and Bruus, H., "Electroosmotic pumping of nonconducting liquids by viscous drag from a secondary conducting liquid", ***Tech Proc Nanotech***, Vol. 1, (2003), 190-193.
27. Ngoma, G.D. and Erchiqui, F., "Pressure gradient and electroosmotic effects on two immiscible fluids in a microchannel between two parallel plates", ***Journal of Micromechanics and Microengineering***, Vol. 16, No. 1, (2005), 83-91.

28. Gao, Y., Wong, T.N., Yang, C. and Ooi, K.T., "Two-fluid electroosmotic flow in microchannels", ***Journal of Colloid and Interface Science***, Vol. 284, No. 1, (2005), 306-314.
29. Su, J., Jian, Y.-J., Chang, L. and Li, Q.-S., "Transient electro-osmotic and pressure driven flows of two-layer fluids through a slit microchannel", ***Acta Mechanica Sinica***, Vol. 29, No. 4, (2013), 534-542.
30. Gao, Y., Wong, T.N., Yang, C. and Ooi, K.T., "Transient two-liquid electroosmotic flow with electric charges at the interface", ***Colloids and Surfaces A: Physicochemical and Engineering Aspects***, Vol. 266, No. 1, (2005), 117-128.
31. Stiles, T., Fallon, R., Vestad, T., Oakey, J., Marr, D., Squier, J. and Jimenez, R., "Hydrodynamic focusing for vacuum-pumped microfluidics", ***Microfluidics and Nanofluidics***, Vol. 1, No. 3, (2005), 280-283.
32. Fu, L.-M., Yang, R.-J. and Lee, G.-B., "Electrokinetic focusing injection methods on microfluidic devices", ***Analytical chemistry***, Vol. 75, No. 8, (2003), 1905-1910.
33. Afonso, A., Alves, M. and Pinho, F., "Analytical solution of two-fluid electro-osmotic flows of viscoelastic fluids", ***Journal of Colloid and Interface Science***, Vol. 395, (2013), 277-286.
34. Kirby, B.J., "Micro-and nanoscale fluid mechanics: Transport in microfluidic devices, Cambridge University Press, (2010).
35. Kandlikar, S., Garimella, S., Li, D., Colin, S. and King, M.R., "Heat transfer and fluid flow in minichannels and microchannels, elsevier, (2005).

Two-fluid Electrokinetic Flow in a Circular Microchannel

RESEARCH NOTE

A. Jabari Moghadam

Department of Mechanical Engineering, Shahrood University of Technology, Shahrood, Iran

PAPER INFO

Paper history:
Received 29 May 2016
Received in revised form 17 July 2016
Accepted 25 August 2016

Keywords:
Electroosmosis
Pressure-gradient
Two-fluid stratified Flow
Exact Solution

چکیده

جریان دوسیاله، به‌وسیله‌ی اثر ترکیبی نیروی الکترواسموتیک در مایع رسانا و گرادیان فشار در مایع نارسانا ایجاد می‌شود. معادله‌های پواسون–بولتزمن و ناویر–استوکس به صورت تحلیلی حل می‌شوند؛ و اثر پارامترهای حاکم بررسی می‌گردد. عدد پوازی با افزایش پارامترهای درگیر، زیاد می‌شود. دو سیال ،در غیاب گرادیان فشار، پروفیل‌های توپی شکل را به نمایش می-گذارند. از نتایج آشکار می‌شود که دبی پمپاژ الکترواسموتیک دوسیاله، به ازای پتانسیل زتای نسبتا کوچک مرز دو سیال، یا مقادیر بزرگ پتانسیل زتای دیوار و شعاع الکتروسینتیک بزرگ، امکان‌پذیر و قابل دسترسی است. برای مقادیر بخصوصی از پارامترهای حاکم، با میل شعاع الکتروسینتیک به بینهایت، دبی به یک مقدار خاص می‌رسد. به ازای مقادیر به قدر کافی کوچک پتانسیل زتای دیوار یا مقادیر به قدر کافی بزرگ پتانسیل زتای مرز، جریان برگشتی (مقدار منفی برآیند دبی) رخ می‌دهد (حتا در حالت جریان یاری شونده توسط فشار). دبی‌های صفر نیز ممکن است به دست آید.

***doi**: 10.5829/idosi.ije.2016.29.10a.18*